Supporting Information for:

Water Resistant and Flexible MOF Materials for Highly-Efficient Separation of Methane from Nitrogen

Xiao-Wei Liu,[†,§] Yi-Ming Gu,[†,§] Tian-Jun Sun,*[†] Ya Guo,[†,§] Xiao-Li Wei,[†,§] Sheng-Sheng Zhao[†] and Shu-Dong Wang*[†]

[†]Dalian National Laboratory for Clean Energy (DNL), Dalian Institute of Chemical Physics (DICP), Chinese Academy of Sciences (CAS), 457 Zhongshan Road, Dalian 116023, P. R. China

[§]University of Chinese Academy of Sciences (UCAS), 19 A Yuquan Road, Beijing 100049, P. R. China

Email: wangsd@dicp.ac.cn, suntianjun@dlmu.edu.cn

Contents:

S1. Supporting Figures and Tables

S2. References

Supporting Figures and Tables

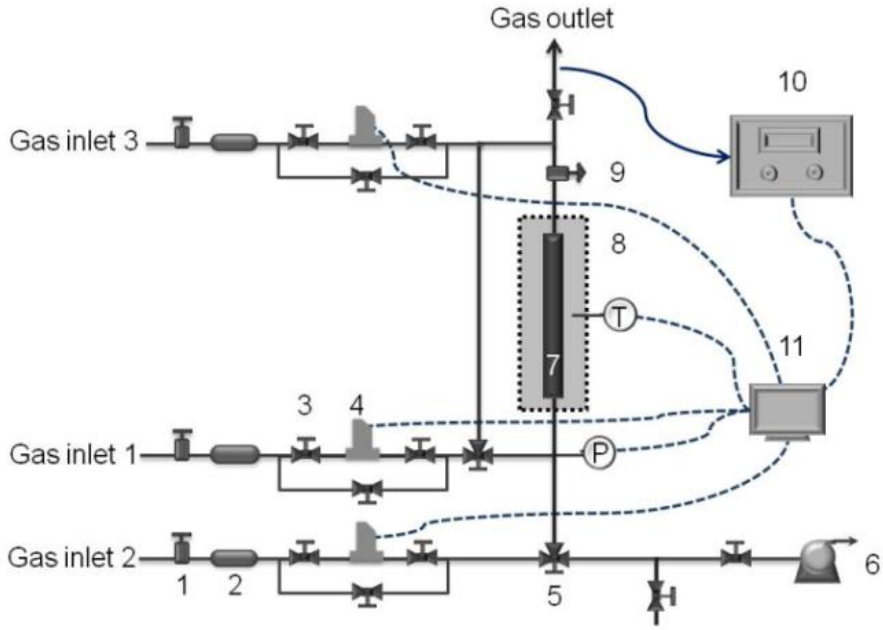

Figure S1. Schematic of the set-up for breakthrough experiments. 1. pressure reducing regulator; 2. gas purifier; 3. two-way valve; 4. mass flowmeter; 5. three-way valve; 6. vacuum pump; 7. adsorbent fixed-bed; 8. thermostatic chamber; 9. back pressure regulator; 10. mass spectrometer; 11. computer.

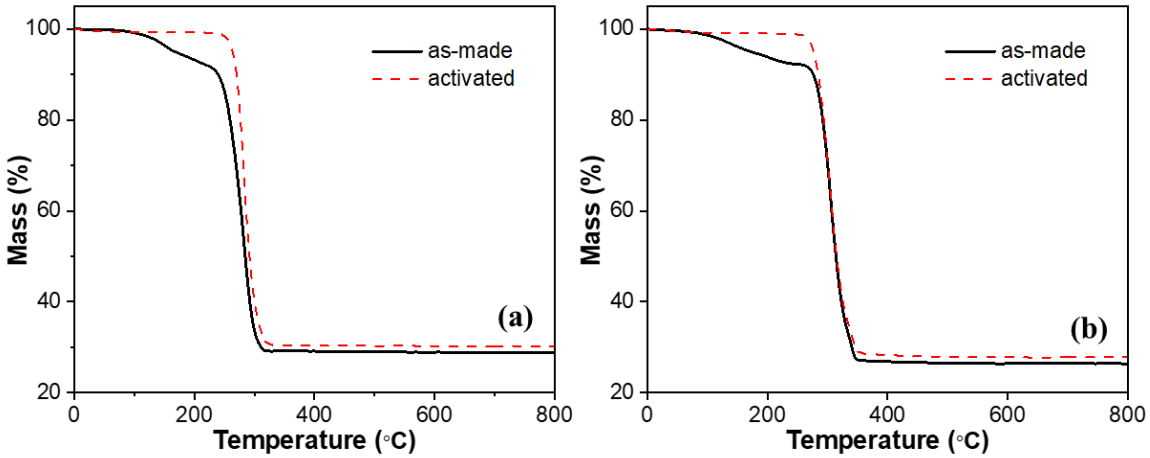

Figure S2. TGA patterns of **(a)** Co-MA-BPY and **(b)** Ni-MA-BPY MOFs: the as-made (black solid line) and the guest-free (red dash line) samples.

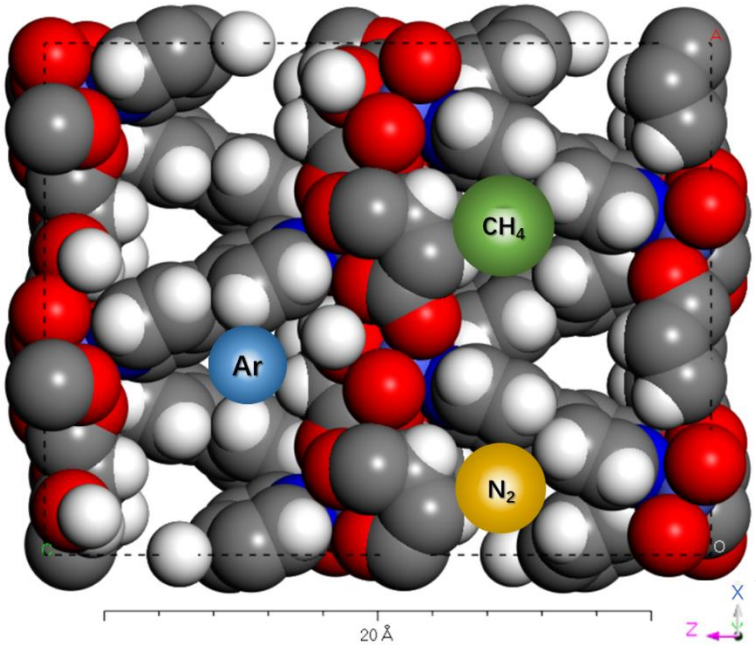

PLD of Co-MA-BPY: 2.5 Å

PLD of Ni-MA-BPY: 3.0 Å

Kinetic diameter of Ar (3.4 Å), CH_4 (3.8 Å) and N_2 (3.6 Å)

Figure S3. Schematic showing larger gas molecules inaccessible to the pore channels of M-MA-BPY MOFs of the original state.[1] Key of atoms: Co or Ni (pale blue), C (grey), O (red), N (blue) and H (white).

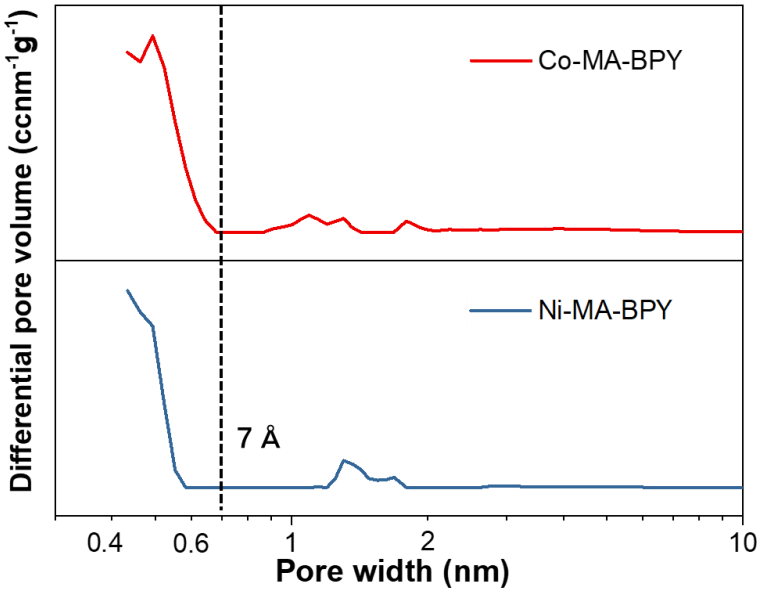

Figure S4. Pore size distributions (PSDs) of Co-MA-BPY (red solid line) and Ni-MA-BPY (blue dash line) MOFs. PSDs are calculated by using a NLDFT cylindrical pores model.

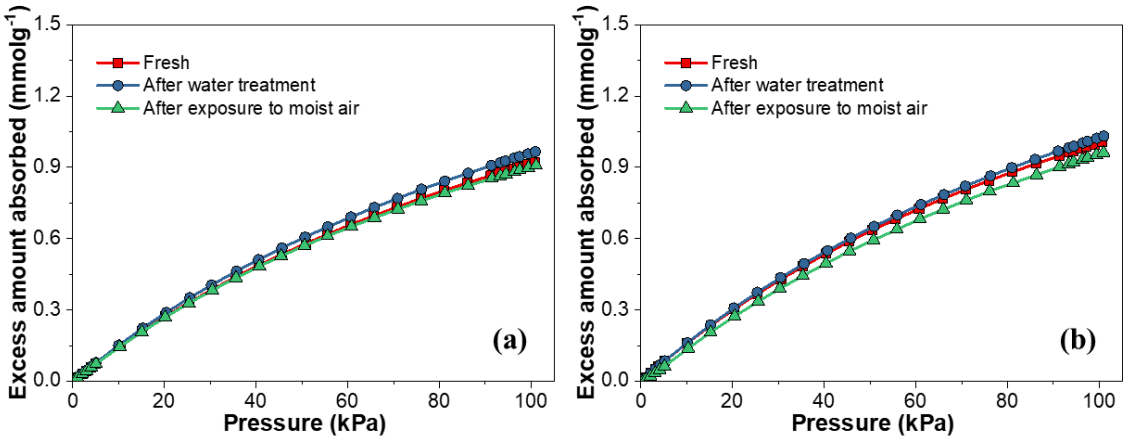

Figure S5. Pure CH_4 adsorption isotherms of different **(a)** Co-MA-BPY and **(b)** Ni-MA-BPY MOF samples at 298 K: fresh (red squares), after being soaked in water for 24 h (blue circles) and after being exposed to 75% RH air atmosphere for 2 weeks (green triangles).

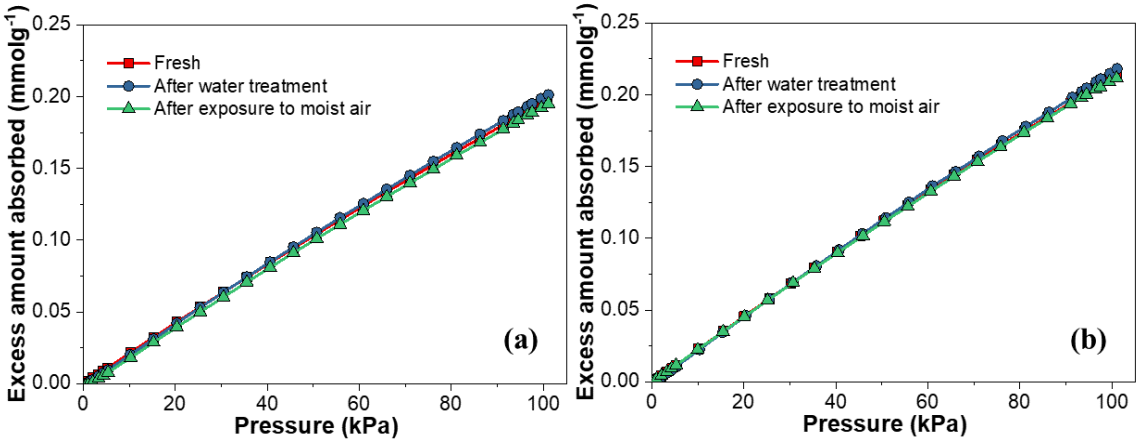

Figure S6. Pure N_2 adsorption isotherms of different **(a)** Co-MA-BPY and **(b)** Ni-MA-BPY MOF samples at 298 K: fresh (red squares), after being soaked in water for 24 h (blue circles) and after being exposed to 75% RH air atmosphere for 2 weeks (green triangles).

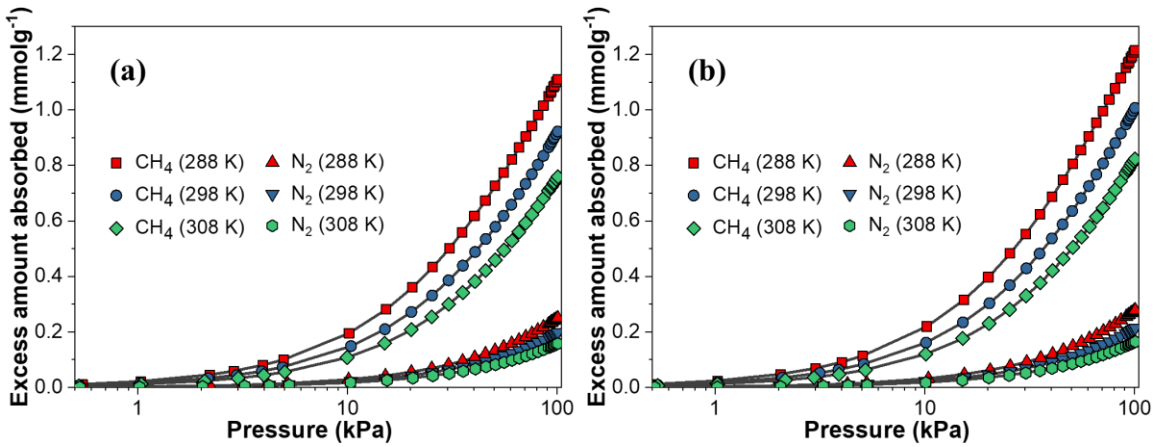

Figure S7. Pure CH_4 (squares, circles and diamonds) and N_2 (triangles and hexagons) adsorption isotherms of **(a)** Co-MA-BPY and **(b)** Ni-MA-BPY MOF samples at 288 (red), 298 (blue) and 308 K (green) based on a x-logarithmic scale. Black lines indicate the dual sites Langmuir-Freundlich fitting data.

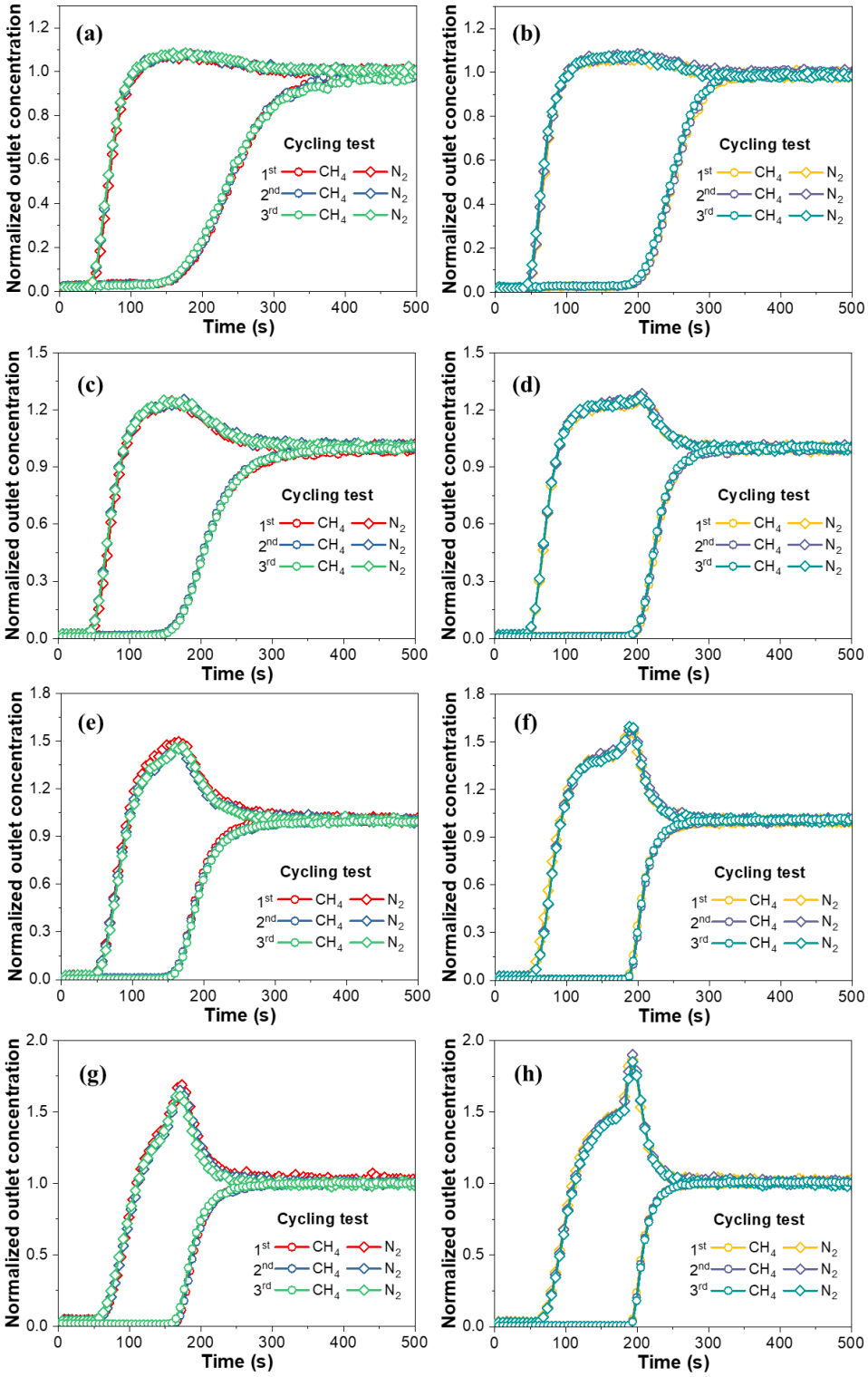

Figure S8. Experimental column breakthrough curves of cycling tests for CH_4/N_2 binary mixtures with different compositions (v/v) **(a, b)** 5: 95, **(b, d)** 15: 85, **(e, f)** 30: 70 and **(g, h)** 50: 50 in an absorber bed packed with Co-MA-BPY **(a, c, e** and **g)** and Ni-MA-BPY **(b, d, f** and **h)** at 298 K and 1.0 bar.

Table S1. Textual properties of the porous structures of M-MA-BPY (M=Co and Ni) MOFs characterized using Zeo++ software package based on the reported structures[1] and calculated from their experimental argon adsorption isotherms at 87 K.

Adsorbents	*LCD*[a] (Å)	*PLD*[a] (Å)	S_{BET} ($m^2\ g^{-1}$)	$S_{Langmuir}$ ($m^2\ g^{-1}$)	V_t[b] ($cm^3\ g^{-1}$)	V_{mic}[c] ($cm^3\ g^{-1}$)
Co-MA-BPY	5.223	2.520	451	575	0.230	0.142
Ni-MA-BPY	5.098	3.022	464	544	0.191	0.160

[a] LCD and PLD were characterized using the open-source Zeo++ software package, [b] V_t (total pore volume) was calculated by Gurvich-rule at P/P_0=0.95, [c] V_{mic} (micropore volume) was calculated by t-Plot method. Here micropore suggests the pores with a diameter smaller than 2.0 nm.

Table S2. Fitting parameters of the DSLF model for CH_4 and N_2 adsorption on Co-MA-BPY MOF at different temperature

Adsorbates	CH_4	N_2	CH_4	N_2	CH_4	N_2
T/K	288	288	298	298	308	308
q_1 (mmol g^{-1})	2.2543	1.5286	2.1688	1.5283	2.0377	1.5865
b_1 (kPa^{-1})	9.1332E-03	1.3797E-03	6.7964E-03	1.0395E-03	5.1956E-03	7.3382E-04
c_1	0.9937	0.9919	0.9995	0.9848	1.0095	1.0056
q_2 (mmol g^{-1})	0.8882	0.8883	0.8715	0.8524	0.8424	0.7656
b_2 (kPa^{-1})	8.9575E-04	8.8943E-04	8.8119E-04	8.6464E-04	8.5628E-04	7.9892E-04
c_2	0.8822	0.9889	0.8696	0.9738	0.8635	0.9459

Table S3. Fitting parameters of the DSLF model for CH_4 and N_2 adsorption on Ni-MA-BPY MOF at different temperature

Adsorbates	CH_4	N_2	CH_4	N_2	CH_4	N_2
T/K	288	288	298	298	308	308
q_1 (mmol g^{-1})	2.3736	1.9444	2.2537	1.4343	2.1201	1.2401
b_1 (kPa^{-1})	9.6882E-03	1.2335E-03	7.1805E-03	1.1617E-03	5.4622E-03	9.7995E-04
c_1	0.9979	0.9929	1.0069	0.9997	1.0152	0.9957
q_2 (mmol g^{-1})	0.9059	0.8936	0.8764	0.8637	0.8592	0.8092
b_2 (kPa^{-1})	8.8772E-04	8.9472E-04	8.8462E-04	8.6710E-04	8.7192E-04	8.5242E-04
c_2	0.8975	0.9858	0.8799	0.9774	0.8593	0.9577

Table S4. Selectivities of CH_4/N_2 and the CH_4 sorption capacity of some selected adsorbents at 298 K and 1 bar.

Adsorbents	Selectivity (CH_4/N_2 50:50, v/v)	CH_4 Capacity (mmol g^{-1})	Ref.
Co-MA-BPY	7.16	0.92	This work
Ni-MA-BPY	7.41	1.01	This work
Zeolite-5A	0.94	0.81	2
MOF-5	1.13	0.13	2
Cu(me-4py-trz-ia)	4.20	1.12	3
ATC-Cu	9.70	2.90	4
HKUST-1	3.70	0.90	4
$Ni_3(HCOO)_6$	6.20	0.78	5
$Co_3(HCOO)_6$	5.50	0.79	6
$Cu(INA)_2$	6.90	0.83	7
$Co_3(C_4O_4)(OH)_2$	12.50	0.40	8
USTA-30a	5.00	0.63	9
Cu-MOF	6.90	0.47	10
Ni-MOF-74	3.80	1.91	11
Co-MOF-74	3.20	1.63	11
Mg-MOF-74	1.50	1.66	11

Reference

1. Duan, L.-M.; Xie, F.-T.; Chen, X.-Y.; Chen, Y.; Lu, Y.-K.; Cheng, P.; Xu, J.-Q., Syntheses, structures, and magnetic properties of three novel metal-malate-bipyridine coordination polymers with layered and pillared topology. *Cryst. Growth Des.* **2006,** *6* (5), 1101-1106.
2. Saha, D.; Bao, Z.; Jia, F.; Deng, S., Adsorption of CO_2, CH_4, N_2O, and N_2 on MOF-5, MOF-177, and Zeolite 5A. *Environ. Sci. Technol.* **2010,** *44* (5), 1820-1826.
3. Möllmer, J.; Lange, M.; Möller, A.; Patzschke, C.; Stein, K.; Lässig, D.; Lincke, J.; Glässer, R.; Krautscheid, H.; Staudt, R., Pure and mixed gas adsorption of CH_4 and N_2 on the metal-organic framework Basolite®A100 and a novel copper-based 1,2,4-triazolyl isophthalate MOF. *J. Mater. Chem.* **2012,** *22* (20), 10274-10286.
4. Niu, Z.; Cui, X.; Pham, T.; Lan, P. C.; Xing, H.; Forrest, K. A.; Wojtas, L.; Space, B.; Ma, S., A metal-organic framework based methane nano-trap for the capture of coal-mine methane. *Angew. Chem. Int. Ed.* **2019,** *https://doi.org/10.1002/anie.201904507*.
5. Liu, X.-W.; Guo, Y.; Tao, A.; Fischer, M.; Sun, T.-J.; Moghadam, P. Z.; Fairen-Jimenez, D.; Wang, S.-D., "Explosive" synthesis of metal-formate frameworks for methane capture: an experimental and computational study. *Chem. Commun.* **2017,** *53* (83), 11437-11440.
6. Hu, J.; Sun, T.; Liu, X.; Zhao, S.; Wang, S., Rationally tuning the separation performances of $[M_3(HCOO)_6]$ frameworks for CH_4/N_2 mixtures via metal substitution. *Micropor. Mesopor. Mater.* **2016,** *225*, 456-464.
7. Hu, J.; Sun, T.; Liu, X.; Guo, Y.; Wang, S., Separation of CH_4/N_2 mixtures in metal-organic frameworks with 1D micro-channels. *RSC Adv.* **2016,** *6* (68), 64039-64046.
8. Liangying, L.; Lifeng, Y.; Jiawei, W.; Zhiguo, Z.; Qiwei, Y.; Yiwen, Y.; Qilong, R.; Zongbi, B., Highly efficient separation of methane from nitrogen on a squarate-based metal-organic framework. *AlChE J.* **2018,** *64*, 3681-3689.
9. He, Y.; Xiang, S.; Zhang, Z.; Xiong, S.; Fronczek, F. R.; Krishna, R.; O'Keeffe, M.; Chen, B., A microporous lanthanide-tricarboxylate framework with the potential for purification of natural gas. *Chem. Commun.* **2012,** *48* (88), 10856-10858.
10. Wu, X.; Yuan, B.; Bao, Z.; Deng, S., Adsorption of carbon dioxide, methane and nitrogen on an ultramicroporous copper metal-organic framework. *J. Colloid Interf. Sci.* **2014,** *430*, 78-84.
11. Li, L.; Yang, J.; Li, J.; Chen, Y.; Li, J., Separation of CO_2/CH_4 and CH_4/N_2 mixtures by M/DOBDC: A detailed dynamic comparison with MIL-100(Cr) and activated carbon. *Micropor. Mesopor. Mater.* **2014,** *198*, 236-246.